

Investigation of surface roughness effects on fluid flow in passive micromixer

Gaurav Pendharkar · Raghavendra Deshmukh ·
Rajendra Patrikar

Received: 22 July 2013 / Accepted: 19 October 2013 / Published online: 7 November 2013
© Springer-Verlag Berlin Heidelberg 2013

Abstract Surface roughness effects are dominant at microscale. In this study, microchannels are fabricated on Silicon substrate. The roughness morphology is modeled for the fabricated structure using Weierstrass-Mandelbrot function for self-similar fractals. A two dimensional model of hexagonal passive micromixer is analyzed with surface roughness present on inner walls of channels using parallel Lattice Boltzmann method, implemented on sixteen node cluster. The results are compared by simulating this micromixer structure using Navier–Stokes equations. The experimental results on the fabricated micromixers are also presented. The effects of relative roughness, fractal dimension and Reynolds number are discussed on laminar flow in hexagonal passive micromixers. The study concludes the importance of modeling surface roughness effect for better mixing efficiency.

1 Introduction

Microfluidics study is important for implementing Lab-on-chips. Micromixers are very important components on these chips. The increasing surface to volume ratio (S/V) at micro and nanoscale of these devices, triggered interest amongst researchers because of its effect on the mixing processes.

Micromixers can be broadly classified into active micromixers and passive micromixers. Active micromixers are based on disturbances caused by external fields. The external energy can be thermal (Tsai and Lin 2002), Acoustic (Yaralioglu et al. 2004), Magneto-hydrodynamic (Bau et al.

2001), Pressure (Okkels and Tabeling 2004), Electric field (Daghighi and Li 2013). Active micromixers have high mixing efficiency at faster rate than passive micromixers. However, due to complex geometrical design and possibility of biochemical reactions due to applied forces, they are not preferred.

Passive micromixers rely on molecular diffusion and chaotic advection for mixing. Passive micromixers with different geometrical constructions like T-micromixer (Wong et al. 2004), Y-micromixers for enhancing particle dispersion (Bhagat and Papautsky 2008), micromixer based on unbalanced splits and collision of fluid streams (Ansari et al. 2010) are also reported. Passive micromixers are biochemically safer and easier to integrate on microchips. The optimization of the micromixer geometrical structure improves mixing performances. Considerable work has been done towards improvement of mixing efficiency, mixing lengths and other parameters.

Effect of surface roughness on microfluidic flow analysis is not a much explored, although it is important parameter since the surface to volume ratio is increasing with miniaturization. The effect of surface roughness is also required to be accurately modeled. These models are required in design and analysis of these components. The simulation studies of rough surfaces were done by randomly generated peaks (Croce and D'Agaro 2005), porous media (Klein-streuer and Koo 2004), and Gaussian distribution (Bahrami et al. 2006). The above simulation studies provide important information about fluid flow on rough surfaces. The physical roughness of the surface depends on the substrate, deposition and etch processes. This roughness measurement can be represented by its frequency properties and by power spectrum. Instruments with different resolutions and scan lengths yield different values of these statistical parameters for these surfaces (Patrikar 2004). The fractal

G. Pendharkar (✉) · R. Deshmukh · R. Patrikar
MiNaG, Department of Electronics, VNIT, Nagpur, India
e-mail: g.pendharkar@iieee.org

models are used to describe the surfaces. Fractals help to model spatial variation through Weierstrass-Mandelbrot function. Lattice Boltzmann modeling gives flexibility to model complex fluid flows as compared to Navier–Stokes equation. Also, the incorporation of surface roughness is comparatively easy because of its grid like structure. For benchmarking of results, we have simulated the structure with Navier–Stokes equation.

Rest of the paper is organized as follows. This study uses fractal geometry to model the hexagonal passive micromixers as explained in Sect. 2. Lattice Boltzmann model along with self-similar fractal based model called Weierstrass-Mandelbrot function is explained in Sect. 3. This section also discusses the fabrication of hexagonal passive micromixer (HPM) and test setup with characterization methodology. Investigations are carried out on velocity profile of fluid, self-affine fractals on Reynolds number, mixing efficiency and roughness effect on mixing length as explained in Sect. 4. Section 5 concludes with observations from simulations and experimental verifications of effect of surface roughness as an added advantage for better mixing performance.

2 Micromixer modeling

A huge cost of fabrication has resulted in use of CAD tools for modeling and optimization of designs. The Lattice Boltzmann modeling carries advantages like parallelization, complex geometrical structures etc. over currently used Navier–Stokes (NS) equation to solve fluid flows. In this work, the modeled microchannels are sufficiently large where NS could also model fluid flows. But, in small nanochannels, due to the strong confinement, the wall may affect the flow greatly through some microscopic parameters, such as the fluid–wall molecular binding energy (Heinbuch and Fischer 1989; Sun and Ebner 1992; Barrat and Bocquet 1999; Zhu and Granick 2002). The fluid flow parameters at macro and microscale may combine and lead to a new phenomenon like the inhomogeneity between the fluid density and viscosity, the boundary condition at the fluid–wall interface can vary from slip to multilayer sticking with the change of fluid–wall binding energy (Travis et al. 1997). We, thus believe, correct roughness model for boundary walls with Weierstrass-Mandelbrot function and the correct fluid flow modeling technique by Lattice Boltzmann method is helpful in predicting correct flow parameters.

2.1 Lattice Boltzmann method

Lattice Boltzmann method (LBM) is a recent mesoscopic technique that solves for a single particle velocity

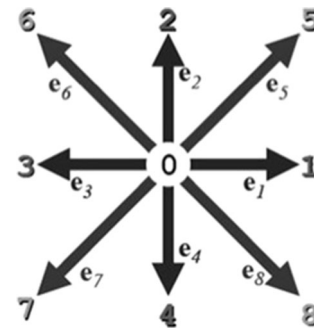


Fig. 1 D2Q9 model of Lattice Boltzmann model (Sauro Succi 2001)

distribution function in a discretized time and space domains (Sauro Succi 2001). The Lattice Boltzmann method is a two-step process. It involves streaming and collision of particles to the local lattice points of the model. LBM has several advantages over conventional computational fluid dynamics (CFD) methods like-dealing with complex boundaries, incorporation of microscopic interactions, and parallel computation.

The fluid flow is usually visualized and solved in 2 Dimension (2D). The grid is made of particles, which act as lattice points. A discrete velocity for a particle in a 2D structure (D2Q9: 2 Dimensional, 9 velocities) is shown in Fig. 1. The arrows indicate the magnitudes and directions of the allowed velocities e_i a lattice site. The LBM is two steps process—(i) Collision, in this step the redistribution of the distribution functions computed (based on existing density and velocity at a given lattice node) and (ii) Streaming, in this step propagation of these distribution functions computed (in the corresponding lattice directions). On solving this, all hydrodynamic quantities are obtained as velocity moments of these distribution functions of different order. The LBM calculations for a particle are local in nature, and hence the computations are highly parallelizable as well as solving for complex boundaries and multi-component mixtures is easy.

The Boltzmann equation can be written as

$$\frac{\partial f}{\partial t} = \nu \cdot \nabla f = Q \quad (1)$$

With Bhatnagar-Gross-Krook (BGK) approximation for the collision term on the right hand side of Eq. 1 is elaborated as follows

$$\frac{\partial f}{\partial t} = \nu \cdot \nabla f = -\frac{1}{\tau} (f - f^{eq}) \quad (2)$$

where, τ is the relaxation parameter, ν is kinematic viscosity of fluid. f and f^{eq} are distribution function and local equilibrium distribution function respectively. The

relaxation parameter and kinematic viscosity are related as

$$\nu = \frac{2\tau - 1}{6} \tag{3}$$

After discretizing velocity space in lattice directions i , Eq. 2 is rewritten as

$$\frac{\partial f_i}{\partial t} + v_i \cdot \nabla f_i = -\frac{1}{\tau}(f_i - f_i^{eq}) \tag{4}$$

where, f_i is distribution function for i th lattice. Equation 4 results the working equation for LBM is as follows:

$$f(x + c_i \Delta t, t + \Delta t) = f(x, t) - \frac{1}{\tau}(f_i - f_i^{eq}) \tag{5}$$

with velocity in i th direction c_i , and distance travelled by particle Δx in time Δt . Equation 5 involves both the collision and streaming steps (Sukop and Thorne 2006).

The zero, first and second velocity moments of the distribution function give mass density, momentum, and stress-tensor respectively, as given in the following equations

$$\rho = \sum_i f_i \tag{6}$$

$$\rho u = \sum_i f_i c_i \tag{7}$$

$$\prod \alpha\beta = \sum_i f_i c_{i\alpha} c_{i\beta} \tag{8}$$

The code for the above method was written and verified for standard conditions.

2.2 Surface roughness modeling

The processes used during micro fabrication process results in rough surface. Shrinking size of fluidic channels to micro and nano scales has considerable roughness effects. The roughness of surfaces can be represented by its frequency properties and power spectrum. Instruments with different resolutions and scan lengths yield different values of these statistical parameters for the surface (Patrikar 2004). This problem is solved by using fractal geometry, which gives instrument independent parameter for characterizing surface roughness. Spatial variation is modeled using fractal dimension D defined by Weierstrass-Mandelbrot function.

$$D = \frac{\log n}{\log(1/r)} \tag{9}$$

D is non-integer with value between 1 and 2 and r is the ratio of N parts scaled down from the whole. The rough surface, used in this study is modeled using the Weierstrass-Mandelbrot as follows

$$f(x) = \sum_{n=-\infty}^{\infty} b^{-n(2-D)} [1 - k \cos(b^n x + \vartheta)] \tag{10}$$

where, $f(x)$ the rough profile, b is the frequency multiplier value, it varies typically between 1.1 and 3.0, is a randomly generated phase. The parameter k can be used to alter the profile, usually fixed value of $k = 1$ and $b = 2.0$ are used since surfaces used in most of the technological applications are fairly regular (Sauro Succi 2001).

3 Micromixers—simulations, fabrication, test setup

Hexagonal passive micromixer is studied for the effects of surface roughness on fluid flow. This study is done in three different ways. The HPM is simulated by parallel Lattice Boltzmann method written in UNIX C++. HPM is also fabricated on Silicon substrate for verifying LBM simulation results. The test setup for the hardware is developed. The simulations of HPM are also performed using Navier–Stokes equation with surface roughness effects (implemented in COMSOL Multiphysics) for benchmarking of our code.

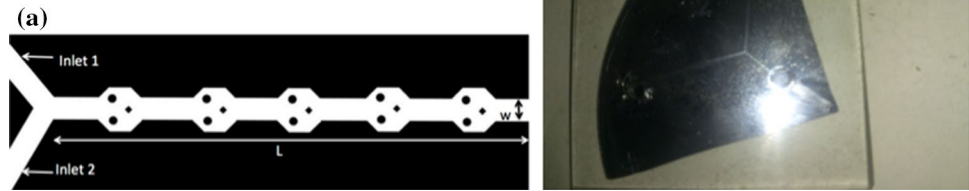
3.1 Lattice Boltzmann simulation

The D2Q9 Parallel Lattice Boltzmann model for the hexagonal passive micromixer is implemented using UNIX C++ and Open MPI. The hexagonal passive micromixer has five hexagonal mixing chambers 400 μm apart. Each mixing chamber has two circular obstacles with diameter 80 μm and one square obstacle with side 70 μm to induce chaotic stirring. The bounce back and periodic boundary conditions are implemented in the stream wise direction by treating nodes on the inflow and outflow as neighbors. A no slip-condition is applied to the wall nodes. The walls of the mixer are made rough with fractal dimension $D = 1.3$ value, as observed in the fabricated microchannels. The parameters for simulations are given in Table 1.

Table 1 LBM simulation parameters

Parameter	Value
Channel dimension	Length: 4.4 mm, Width: 200 μm , Depth: 25 μm
Carrier solution	Inlet 1: mixture of water and glycerol Inlet 2: fluorescent particles
Kinematic viscosity	$7.63 \cdot 10^{-5} \text{ m}^2/\text{s}$
Inlet velocity	0.06 m/s, 30 $\mu\text{l/s}$
Number of lattice points	880×40
Number of time steps	50,000

Fig. 2 **a** Geometry of modeled and fabricated micromixer **b** final chip



3.2 Fabrication of hexagonal passive micromixer

The geometry of micromixer is shown in Fig. 2a. The final chip after bonding is shown in Fig. 2b. The dimensional details of the fabricated design are same as given in LBM simulation stated above.

The fabrication steps for the microchannels are as follows

A RCA cleaned Silicon wafer was used as the substrate material with <110> orientation. Silicon dioxide (SiO_2) with thickness of $1 \mu\text{m}$ was grown by wet oxidation, which acts as a masking layer during etching process. A lithography step for the channel was performed using positive photoresist. This opened the required window for etching channel. The SiO_2 from the opened windows was removed using Buffered HF solution. After removing the photoresist layer, RIE was performed to get the required channel depth. The microchannels were closed by glass plate with Polydimethyl Siloxane (PDMS) as an adhesive between the substrate and glass plate. Details of fabricated microchannels and connectors are given in Table 2.

The reservoirs present at both inlets and outlet are connected to syringe pump with the help of polypropylene tubing. The RMS roughness for the sample was measured by the profilometer. This value is converted to fractal

dimension D by the following process (Majumdar and Tien 1990). A structure functions of AFM image of the sample given by Eq. 11.

$$\begin{aligned} Str(\tau) &= [R(y + \tau) - R(y)]^2 \\ &= \int_{-\infty}^{\infty} s(\omega) (e^{i\omega\tau} - 1) d\omega \\ &= \psi G^{2(D-1)} \tau^{(4-2D)} \end{aligned} \quad (11)$$

The intermediate value ψ is evaluated as

$$\psi = \frac{\Gamma(2D - 1) \sin[(2D - 3)\pi/2]}{2 \ln \gamma (2 - D)} \quad (12)$$

The root mean square roughness height can be represented by following equation

$$\begin{aligned} \sigma &= R^{2.0.5} = \left[\int_{\omega_l}^{\omega_h} s(\omega) d\omega \right]^{0.5} \\ &= \left[\frac{G^{2(D-1)}}{2 \ln \gamma} \frac{1}{4 - 2D} \left(\frac{1}{\omega_l^{(4-2D)}} - \frac{1}{\omega_h^{(4-2D)}} \right) \right]^{0.5} \end{aligned} \quad (13)$$

where $()$ implies temporal average, ψ is a constant, τ is scale, low cut-off frequency $\omega_l = 1/L_s$, L_s sample length, higher frequency $\omega_h = 1/L_r$, L_r resolution of scan instrument, G is scaling constant, D is self-affine fractal dimension γ , scaling parameter for determining the spectral density and self-property.

If the plot of $\log[Str(\tau)]$ vs $\log(\tau)$ is linear, then surface roughness can be represented by self-affine fractal object D . The value of $\gamma = 1.5$ (Majumdar and Tien 1990) for most of the roughness calculations.

3.3 Test setup for fabricated passive micromixer

The test setup for hexagonal passive micromixer consists of a syringe pump, USB Digital microscope, connectors and piping required for fluid flow from syringe pump to microchannels as shown in Fig. 3.

Table 2 Details of microchannel and connectors

	Sample 1	Sample 2	Sample 3
Microchannel length (L)	2.4 mm	3.4 mm	4.4 mm
Microchannel width (W)	200 μm	200 μm	200 μm
Microchannel depth (D)	15 μm	20 μm	25 μm
Processing parameters for reactive ion etching (RIE)	Frequency: 15.59 MHz; gas: SF_6 , flow rate: 25 sccm; RF power: 400 W; load position: 45 %, tune position: 30 %		
Etch rate	3.5 $\mu\text{m}/\text{min}$		
Connectors for microchannels	Type: straight connectors of polypropylene with ID: 1 mm, OD 1.58 mm		

Fig. 3 Characterization setup for the hexagonal passive micromixer

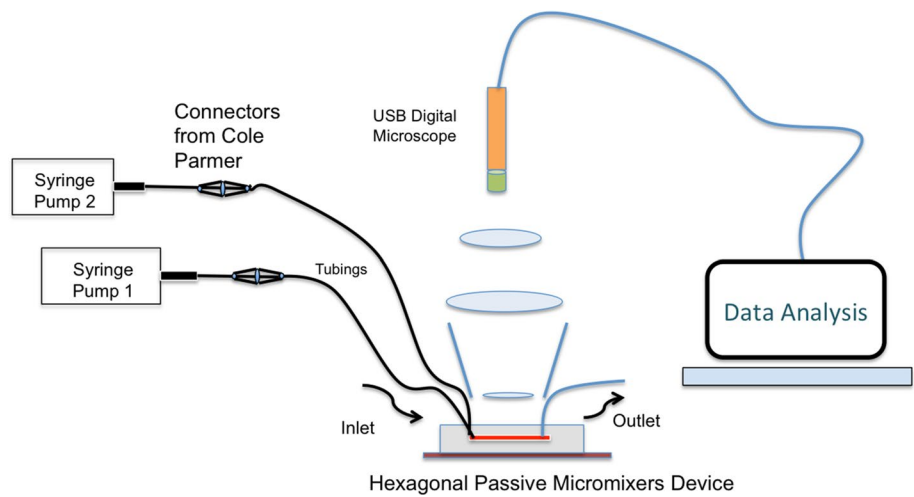


Table 3 COMSOL multiphysics simulation parameters

Parameter	Model 1	Model 2	Model 3
Channel length (L)	2.4 mm	3.4 mm	4.4 mm
Channel width (W)	200 μm	200 μm	200 μm
Carrier solution	Mixture of water and glycerol		
Kinematic viscosity	7.63*10 ⁻⁵ m/s		
Inlet velocity	0.06 m/s, 30 μl/s		
Type of meshing	Free triangular (maximum element size: 0.03)		
Type of study	Time dependent		
Number of nodes	63,587		

The mixing chamber is observed under a Digital microscope with fluorescent particles. The flow rate is set at 30 μl/s. The fluorescent particles are inserted through one end of the channel and flow is continuously observed with digital microscope capturing images at 30 frames per second under the presence of UV light source. The captured frames are post-processed using ImageJ software. The fluid flow is then observed for vorticity and X–Y component of velocities through microchannel during post processing.

3.4 Navier–Stokes equation simulations

A 2D model of passive hexagonal micromixer is designed in COMSOL Multiphysics. Surface roughness on the channel walls is defined by Weierstrass-Mandelbrot model. The simulation parameters are shown in Table 3.

4 Results

Results of simulation and characterization of Micromixer are presented in this section.

4.1 Surface roughness profile

Surface roughness, modeled using Weierstrass-Mandelbrot function for Fractal dimension (D) using Eq. 10 are shown in Fig. 4.

The roughness profile with higher fractal dimension has more frequent variations along the profile. For the fabricated structure, plot of $\log[Str(\tau)]$ vs $\log(\tau)$ is shown in Fig. 5. The linear relation is found with the value of fractal dimension is $D = 1.3$.

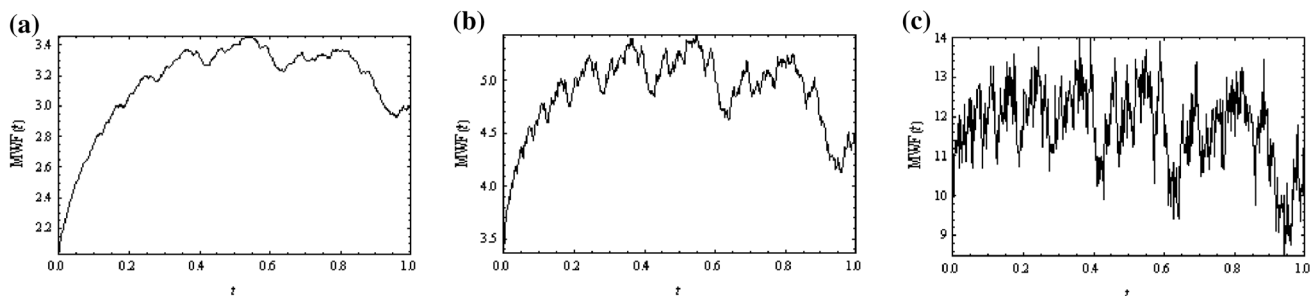


Fig. 4 Simulated fractal surface profiles with various fractal dimension (D) values **a** D = 1.3 **b** D = 1.5 **c** D = 1.8

Fig. 5 **a** AFM image of microchannel **b** Graph between $\log(\tau)$ and $\log [Str(\tau)]$ for the fabricated structures

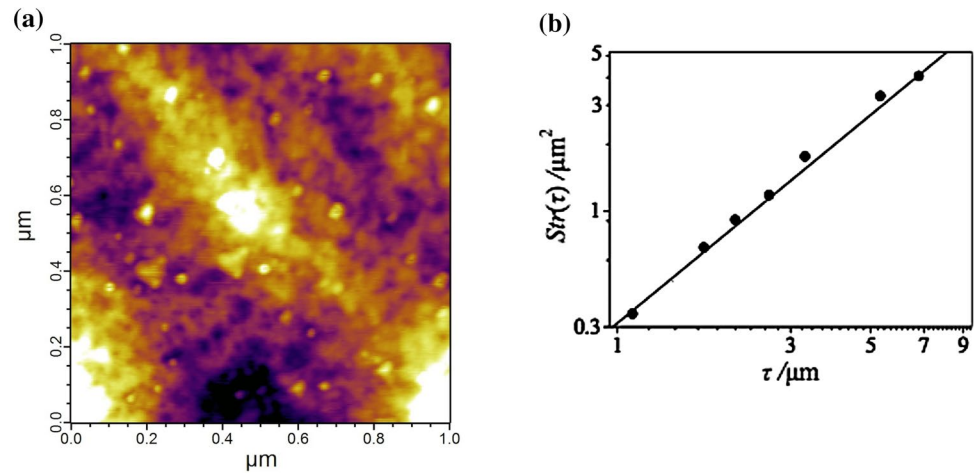


Fig. 6 LBM simulation of Swirls formation at **a** first hexagonal chamber at $L = 500 \mu\text{m}$ **b** third hexagonal mixing chamber at $L = 2,400 \mu\text{m}$

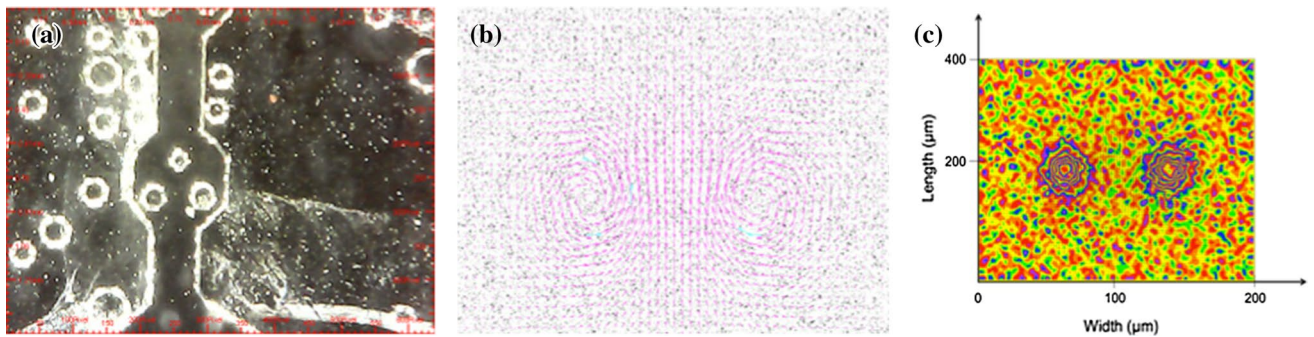
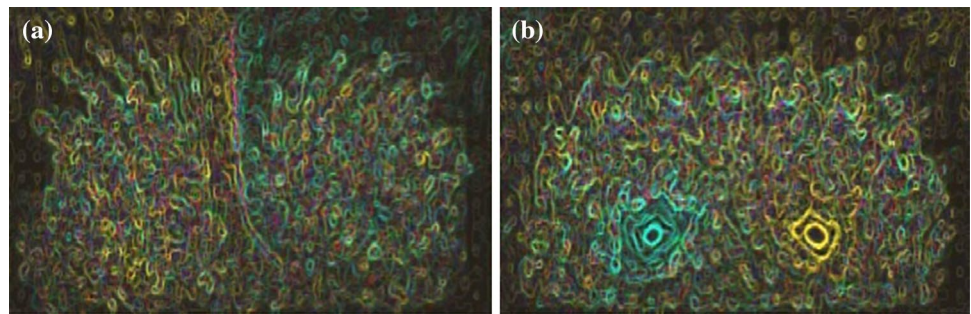


Fig. 7 **a** Experimental observations of passive micromixers chamber at $L = 2,400 \mu\text{m}$ with area $400 \mu\text{m}^2$ **b** Swirls produced after the fluid with tracer particles is passing through the microchannels. **c** Intensity traces of particles across the mixing chamber

4.2 Swirls generated inside mixing chamber

Figure 6 shows the fluid flow across hexagonal mixing chambers simulated using Lattice Boltzmann Method. Figure 7 shows the actual flow profile in the fabricated structure.

The fluids enter the inputs, and this particle stream passes through hexagonal chambers where the flow is disturbed due to the presence of obstacles. The obstacles are placed in such a way that the fluid produces swirls. The

simulated results at the length of $2,400 \mu\text{m}$ are shown in Fig. 6b. The experimental results for the similar situation are shown in Fig. 7c. Both the observations confirm formation of swirls. The direction and size of the swirls match quite well.

4.3 Fluid flow analysis

The fluid flow through the microchannel is analyzed. The pressure gradient at walls is higher due to swirl formation.

Fig. 8 Experimental observation of velocity components for fluid flow **a** U-component of velocity and **b** V-component of velocity

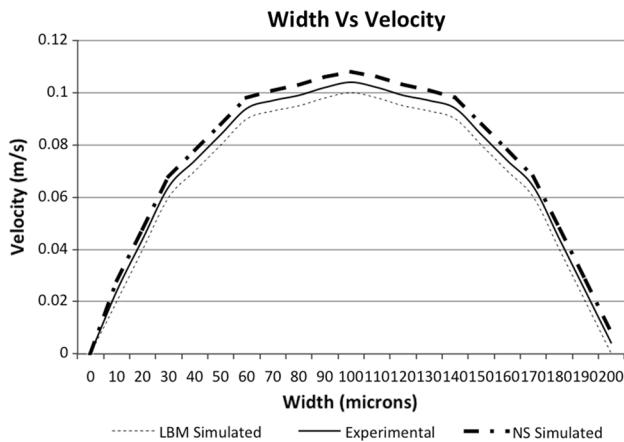
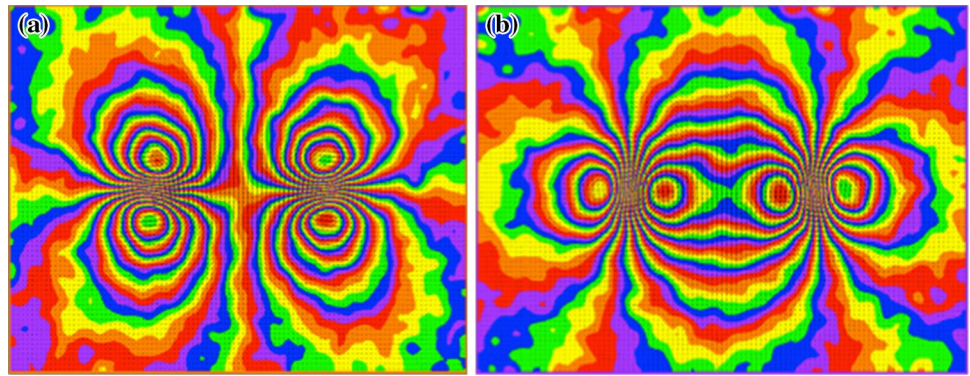


Fig. 9 Fluid flow profile through inlet channel of width 200 μm showing Poiseuille nature

Due to roughness present at the walls, the flow gets perturbed which is studied from the U–V velocity vector components as shown in Fig. 8.

Velocity components of movement of fluid inside the hexagonal mixing chamber are shown in Fig. 8. Figure 8a shows the swirls produced along U component at the center of the chamber show the mixing process. The Fig. 8b

shows component along the axial length of the micromixer. It shows that fluid progressing towards output port. The red color represents maximum intensity of fluid velocity.

The profile of velocity vs channel width for $L = 4.4 \text{ mm}$ is presented in Fig. 9. The experimental observations of the fluid flow through microchannel have parabolic nature with velocity going to peak at center of the channel at width equal to 100 μm . This is modeled as Poiseuille flow (Sukop and Thorne 2006). Simulation results of NS and LBM of the velocity profile with Poiseuille model also confirm the experimental observations.

4.4 Effect of fractal dimension on pressure drop

The presence of roughness changes the velocity of fluid inside the channel. This changes the pressure drop across the channel. Figure 10 shows the graph between channel length and pressure drop for different values of fractal dimension D evaluated using LBM.

It can be observed from Fig. 10 as roughness goes on increasing, the pressure drop increases for same channel length. The pressure drop can be predicted using fractal dimension D . The reason for pressure drop can be explained in detail by considering flow behavior at the channel walls, explained in the next subsection.

Fig. 10 Pressure drop across channel for different D using LBM simulations

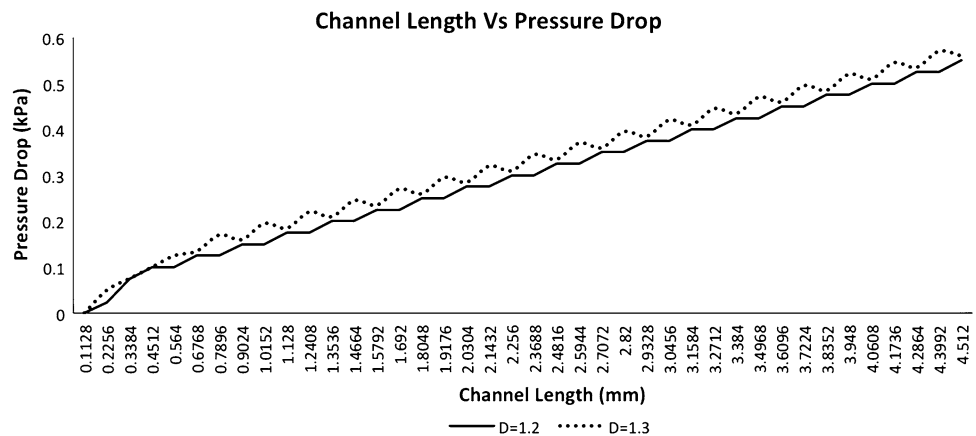
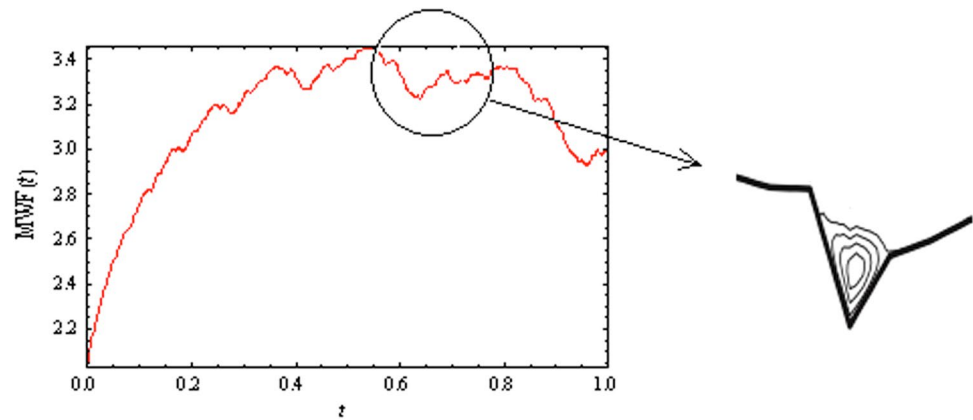


Fig. 11 Vortex observed in LBM simulations at the rough walls



4.5 Flow behavior at channel walls

Fluid flowing inside the microchannel has a velocity profile observed in cross section taken along the channel length. This flow is laminar. This is caused due to the presence of surface roughness at the walls. This is observed when no slip boundary condition is applied during simulations. Figure 11 shows the swirl formation at the rough walls.

The vortices are formed and can be prominently seen at the valley. The flow gets disturbed due to the presence of peaks and valleys. This contributes to increase in the pressure drop. This implies that presence of rough elements result in counter pressure distribution near the surface. Increased swirl effects were observed for high Reynolds number. This is due to presence of roughness at the surface of the channel wall.

4.6 Effect of Reynolds number on mixing efficiency

It can be seen that that when fluid enters very first hexagonal mixing chamber, mixing process starts. It is experimentally observed that the mixing efficiency goes nearly to 70 % at a length equal to 2,400 μm . Mixing efficiency is calculated by taking probability distribution function of mixing images (Nam-Trung Nguyen 2008).

The sample under test has values of RMS roughness of 400 nm. This gives fractal dimension of $D = 1.3$ obtained from Eqs. (11), (12), (13). On the basis of simulations performed in this study and the experimental verification under standard test conditions, it has been found that Reynolds number has value from 0.1 to 0.5, for the system under consideration. The effect of Reynolds number on mixing efficiency as observed in experimental setup and predicted in simulations is shown in Fig. 12.

It is observed that presence of surface roughness improves the mixing efficiency by almost 10 % for Reynolds number from 0.1 to 0.5, after which there is negligible effect of presence of surface roughness on mixing efficiency.

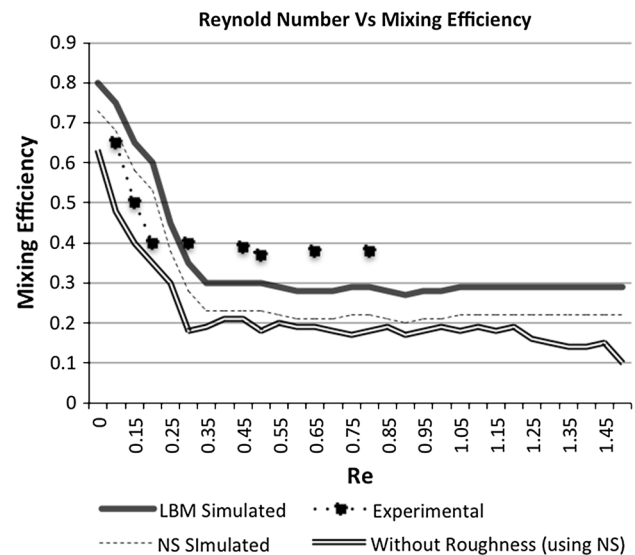


Fig. 12 Reynolds number vs. mixing efficiency for $D = 1.3$, $L = 4.4$ mm

It is also observed that, the fluid mixing occurs due to diffusion and chaotic advection (George Karniadakis et al. 2005). As the Reynolds number is increased, the time for the mixing and advection is less, which results in decreased mixing efficiency. This is observed in Fig. 12 as decrease in the mixing efficiency till Reynolds number of 0.2–0.3. After this, as the Reynolds number is increased, the mixing efficiency is constant and is dependent mainly on the concentration of fluids (George Karniadakis et al. 2005).

5 Conclusion

A 2D model of hexagonal passive micromixer is developed using Lattice Boltzmann method (LBM) for numerical analysis. It is proved from the experimental data that the surface roughness on most of microfabricated surface can be well modeled using Weierstrass-Mandelbrot function.

A detailed study on fluid flow observed swirl formation inside mixing chamber with fluid progressing along axial length as seen from the velocity components. Velocity components from the experimental observations in U–V direction indicate that the flow is disturbed by the presence of obstacles situated at the center of the mixing chamber while the fluid, which is flowing nearby walls, faces increase in pressure gradient due to vortex formation. The velocity profiles in the experimental setup matches well with the simulations in LBM and NS in terms of the values as well as the nature of parabolic curve. This gives us confidence to model the fluid flow in microchannels as Poiseuille flow.

We have observed in simulations that fractal dimension (D), can be effectively used to predict the pressure drop in presence of roughness irregularities in the channel walls since the presence of roughness at the channel walls result in counter pressure distribution near the surface. This may help to predict the optimum permissible values of roughness for efficient mixing since which can be verified by further experimental studies.

We conclude that mixing efficiency can be increased by intentionally adding roughness to the micromixer geometry by adjusting etching parameters. However, for higher fractal dimensions, there is considerable increase in pressure drop. Thus there is need to find optimum value of fractal dimension where one can get maximum mixing efficiency with minimum pressure drop. The values of mixing efficiency and pressure drop also depend on the fluid parameter such as density, viscosity, channel dimensions, inlet velocity (which affect the Reynolds number) which needs a separate study whenever these parameters are changed.

Finally we observe that parallel lattice Boltzmann algorithm, because of its grid like structure can be effectively used to model the fluid flows over a wide range of channel dimensions by incorporation of surface roughness modeled using fractal geometries.

Acknowledgments The authors would like to thank VNIT for their continued support. Authors would like to thank ADA for providing the necessary CAD tools through NPMASS initiative. Authors are grateful to CEN, IIT Bombay and Department of Mechanical Engineering, IIT Bombay for providing the opportunity to carry out fabrication of microfluidic devices.

References

Bhagat AAS, Papautsky I (2008) Enhancing particle dispersion in a passive planar micromixer using rectangular obstacles. *J Micromech Microeng* 18: 085005 doi:[10.1088/0960-1317/18/8/085005](https://doi.org/10.1088/0960-1317/18/8/085005)
 Bahrami M, Yovanovich MM, Culham JR (2006) Pressure drop of fully-developed, laminar flow in microchannels of arbitrary cross-section. *J Fluids Eng* 128(5):1036–1044. doi:[10.1115/1.2234786](https://doi.org/10.1115/1.2234786)

Barrat JL, Bocquet L (1999) Large slip effect at a nonwetting fluid–solid interface. *Phys Rev Lett* 82:4671
 Bau HH, Zhong J, Yi M (2001) A minute magneto hydrodynamic (MHD) mixer. *Sens Actuators B* 79(2-3):205–213
 Bhagat A, Papautsky I (2008) Enhancing particle dispersion in a passive planar micromixer using rectangular obstacles. *J Micromech Microeng* 18: 085005. <http://dx.doi.org/10.1088/0960-1317/18/8/085005>
 Croce G, D’Agaro P (2005) Numerical simulation of roughness effect on microchannel heat transfer and pressure drop in laminar flow. *J Phys D Appl Phys* 38:1518–1530
 Daghighi Y, Li D (2013) Numerical study of a novel induced-charge Electrokinetic micromixer. *Anal Chim Acta* 763:28–37
 Karniadakis G, Beskok A, Aluru N (2005) *Microflows and Nanoflows: fundamentals and simulation*. Springer Publication
 Gobby D, Angeli P, Gavriilidis A (2001) Mixing characteristics of T-type microfluidic mixers. *J Micromech Microeng* 11:126–132
 Heinbuch U, Fischer J (1989) Liquid flow in pores: slip, no-slip, or multilayer sticking. *Phys Rev A* 40:1144
 Kleinstreuer C, Koo J (2004) Computational analysis of wall roughness effects for liquid flow in micro-conduits. *J Fluids Eng* 126(1):1–9. doi:[10.1115/1.1637633](https://doi.org/10.1115/1.1637633)
 Li C, Chen T (2005) Simulation and optimization of chaotic micromixer using lattice Boltzmann method. *Sens Actuators B* 106:871–877
 Majumdar A, Tien CL (1990) Fractal characterization and simulation of rough surfaces. *Wear* 136:313–327
 Ansari MA, Kim I K-Y, Anwar K, Kim SM (2010) A novel passive micromixer based on unbalanced splits and collisions of fluid streams. *J Micromech Microeng* 20: 055007. doi:[10.1088/0960-1317/20/5/055007](https://doi.org/10.1088/0960-1317/20/5/055007)
 Nguyen N-T (2008) *Micromixer: fundamentals, design and fabrication*, William Andrew Inc
 Okkels F, Tabeling P (2004) Spatiotemporal resonances in mixing of open viscous fluids. *Phys Rev Lett* 92:038301
 Patrikar R (2004) Modeling and simulation of surface roughness. *Appl Surf Sci* 228:213–220
 Succi S (2001) *The Lattice Boltzmann equation for fluid dynamics and beyond*, Oxford University Press
 Sukop MC, Thorne DT (2006) *Lattice Boltzmann Modeling*, Springer, Berlin
 Sun M, Ebner C (1992) Molecular dynamics study of flow at a fluid-wall interface. *Phys Rev Lett* 69:3491
 Travis KP, Todd BD, Evans DJ (1997) Departure from Navier–Stokes hydrodynamics in confined liquids. *Phys Rev E* 55:4288
 Tsai JH, Lin L (2002) Active microfluidic mixer and gas bubble filter driven by thermal bubble micropump. *Sens Actuat A-Phys* 97–98:665–671
 Wong SH, Ward MCL, Wharton CW (2004) Micro T-mixer as a rapid mixing micromixer. *Sens Actuators B* 100:365–385
 Wu JJ (2000) Simulation of rough surfaces with FFT. *Tribol Int* 33(1):47–58
 Wu Z, Nguyen NT, Huang XY (2004) Non-linear diffusive mixing in microchannels: theory and experiments. *J Micromech Microeng* 14:04. doi:[10.1088/0960-1317/14/4/022](https://doi.org/10.1088/0960-1317/14/4/022)
 Yaralioglu GG, Wygant IO, Marentis TC, Khuri-Yakub BT (2004) Ultrasonic mixing in microfluidic channels using integrated transducers. *Anal Chem* 76(13):3694–3698. doi:[10.1021/ac035220k](https://doi.org/10.1021/ac035220k)
 Yong Shi, Zhao TS, Guo ZL (2006) Lattice Boltzmann method for incompressible flows with large pressure gradients. *Phys Rev E* 73:026704
 Zhu YX, Granick S (2002) Limits of the hydrodynamic no-slip boundary condition. *Phys Rev Lett* 88:106102